

Rearrangement of the vortex lattice due to instabilities of vortex flow

D. Y. Vodolazov^{1,2,*} and F. M. Peeters^{2,†}

¹*Institute for Physics of Microstructures, Russian Academy of Sciences, 603950 Nizhny Novgorod, GSP-105, Russia*

²*Departement Fysica, Universiteit Antwerpen (CGB), Groenenborgerlaan 171, B-2020 Antwerpen, Belgium*

(Received 16 April 2007; published 24 July 2007)

With increasing applied current, we show that the moving vortex lattice changes its structure from a triangular one to a set of parallel vortex rows in a pinning free superconductor. This effect originates from the change of the shape of the vortex core due to nonequilibrium effects (similar to the mechanism of vortex motion instability in the Larkin-Ovchinnikov theory). The moving vortex creates a deficit of quasiparticles in front of its motion and an excess of quasiparticles behind the core of the moving vortex. This results in the appearance of a wake (region with suppressed order parameter) behind the vortex, which attracts other vortices resulting in an effective direction-dependent interaction between vortices. When the vortex velocity v reaches the critical value v_c , quasiphase slip lines (lines with fast vortex motion) appear, which may coexist with slowly moving vortices between such lines. Our results are found within the framework of the time-dependent Ginzburg-Landau equations and are strictly valid when the coherence length $\xi(T)$ is larger or comparable with the decay length L_{in} of the nonequilibrium quasiparticle distribution function. We qualitatively explain experiments on the instability of vortex flow at low magnetic fields when the distance between vortices $a \gg L_{in} \gg \xi(T)$. We speculate that a similar instability of the vortex lattice should exist for $v > v_c$ even when $a < L_{in}$.

DOI: 10.1103/PhysRevB.76.014521

PACS number(s): 74.25.Op, 74.20.De, 73.23.-b

I. INTRODUCTION

In 1976, Larkin and Ovchinnikov¹ (LO) predicted an instability of vortex motion that is related to the deviation of the quasiparticle distribution function from its equilibrium value near the vortex core (for review, see Ref. 2). When the vortex moves with a velocity v , the order parameter ψ in the vortex core varies on a time scale $\tau_{|\psi|} \sim \xi/v$ that can be smaller than the relaxation time of the nonequilibrium quasiparticles τ_{in} (due to inelastic electron-phonon or electron-electron interactions). As a consequence, the quasiparticle distribution function deviates from its equilibrium and it results to a shrinkage of the vortex core at temperatures close to the critical temperature.² This effect is mainly connected with the removal of quasiparticles from the vortex core by the induced electric field³ and, in some respect, is similar to the dynamic enhancement of superconductivity in weak superconducting links.^{3,4}

Analytical calculations made in the “dirty” limit (mean free path length l of the electrons is smaller than the coherence length ξ) predicted a decrease of the viscosity coefficient η of the vortex motion and the existence of a critical velocity $v_c \sim 1/\sqrt{\tau_{in}}$ at which the viscous force $-\eta v$ reaches its maximal value.² Macroscopically, it results into a nonlinear current-voltage characteristic $V \sim I\eta(I)$ with pronounced hysteresis at relatively weak magnetic fields.² Such a behavior was experimentally observed in many low^{3,5-7} and high⁸⁻¹³ temperature superconductors, and quantitative agreement with theory was found. From the experimental value of the critical voltage $V_c = v_c BL$ (B is a magnetic flux induction and L is the distance between voltage leads), the critical velocity v_c and relaxation time τ_{in} were extracted.

We should stress the nontrivial nature of the LO effect. If we use the Bardeen-Stephen expression¹⁴ for the viscosity of the vortex motion, $\eta = \Phi_0^2/2\pi\xi^2\rho_n c$, we find that it actually *increases* if the size of the vortex core decreases (with, for

example, a decrease of the temperature). In the LO theory, the vortex core shrinks and this results in a *decrease* of the viscosity coefficient η . The possible explanation for this contradiction is the failure of the Bardeen-Stephen model for the vortex as a normal cylinder with radius ξ in case of a moving vortex with high enough velocity.

At low temperatures, small changes in the quasiparticle distribution function cannot influence the order parameter.² As a result, nonlinear effects will start at larger electrical fields and they become significant not only in the vortex core but also around the vortex. Effectively, such nonequilibrium effects were described as due to heating of the quasiparticles by the induced electric field up to a temperature larger than the sample and/or phonon temperature. This results in a suppression of the order parameter near the vortex core and the vortex core expands. This effect was used to explain the experimental results on the vortex motion instability at low temperatures for both “dirty”^{7,16-18} and “pure” ($l \gg \xi$) superconductors.¹⁹ In the latter case, the instability occurs due to a logarithmic dependence of the vortex viscosity on the electronic temperature.

Returning to the LO theory, we note that the main assumption here was the uniform distribution of the nonequilibrium quasiparticle distribution function $f(E)$ in the superconductor. (In particular, this leads to a field-independent critical velocity.) From the good *quantitative* agreement between theory and experiment in large magnetic fields, one may conclude that the above condition is well satisfied when the distance between vortices satisfies $a(B) \ll L_{in}$. However, experiments at low magnetic fields showed that this approach fails when $a(B) \sim \sqrt{\Phi_0/B}$ becomes larger than L_{in} .^{6,9,13,15} In Ref. 15, it was proposed that the instability occurs when the nonequilibrium distribution becomes uniform over the superconductor, which is possible if $v_c \tau_{in} \approx a(B)$. This leads to a dependence $v_c \sim \sqrt{1/B}$ at moderate magnetic fields, which was observed in many

experiments.^{6,9,13,15} However, at lower magnetic fields, the critical velocity should behave as $v_c \sim 1/B$ to explain the field-independent value for the critical voltage V_c (Ref. 13) (the same conclusion can be drawn from Fig. 10 of Ref. 3). Note that at these fields, the current induced magnetic field and, consequently, it cannot explain the observed effect.

Despite the large number of experimental works, there is still the fundamental question of what will happen with the vortex structure when the critical velocity is approached and/or exceeded. In the original paper of Larkin and Ovchinnikov, it was assumed that the vortex lattice does not exhibit any structural changes and transits for $v > v_c$ to a state with a resistance close to the normal value (in the current driven regime). However, experiments on low- and high-temperature superconductors showed that another type of behavior is possible. For example, a transition to a state with phase slip lines was experimentally observed in Refs. 20–24 for low-temperature superconductors, and similar I - V characteristics (which were differently interpreted) were observed in high-temperature superconductors in the voltage driven regime.^{16–18} These experimental results support the idea that some kind of phase transition occurs in the vortex lattice at the instability point, and regions with fast and slow vortex motions appear in the sample.^{16–18,20–24}

To answer the above questions theoretically, one should use a rather complicated set of integro-differential equations for the order parameter, Green's functions of the superconductor, and quasiparticle distribution function.² At the present time, it looks almost as an impossible task to solve these equations even numerically. Therefore, we will limit ourselves to the equations that were derived from the microscopic equations for a superconductor in the “dirty” limit under the assumption that the relaxation length $L_{in} = \sqrt{D\tau_{in}}$ of $f(E)$ (D is the diffusion constant) is smaller than the coherence length $\xi(T)$.^{25,26} They are the extended (or generalized) time-dependent Ginzburg-Landau equations and contain explicitly a parameter τ_{in} . From the very beginning, we are in a different limit as compared to the LO theory, because we consider a nonequilibrium $f(E)$ that is nonuniform in the sample. The longitudinal (odd in energy) part $f_L(E) = f(-E) - f(E)$ of the nonequilibrium $f(E)$ distribution (which is actually responsible for the variation of $|\psi|$) is localized only in the region where the time derivative $\partial|\psi|/\partial t$ is finite [see Eqs. (6) and (10) in Ref. 25]. It means that $f_L(E)$ is nonzero only near the moving vortex core.

The paper is organized as follows. In Sec. II, we present our model system. In Sec. III, we study the rearrangement of the vortex structure due to nonequilibrium effects at moderate and high magnetic fields and, in Sec. IV, the nonequilibrium vortex dynamics at zero magnetic field. Finally, in Sec. V, we discuss our results and make a comparison with experiments.

II. MODEL SYSTEM

As a model system, we use a bulk superconductor which is infinite in the z and y directions and is finite in the x direction (see Fig. 1). This model allows us to study the

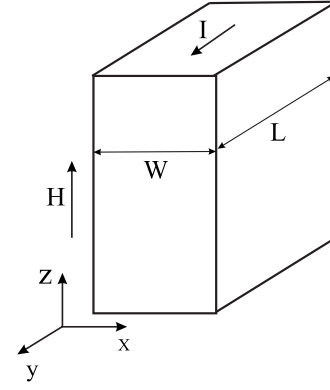


FIG. 1. Model system—a superconducting slab (infinitely long in the y and z directions) in a parallel magnetic field H with transport current I .

effect of the nonuniform current distribution in the superconductor (due to transport current) on the vortex dynamics at zero and low magnetic fields.

In our calculations, we neglect the possibility of the formation of curved vortices in the z direction and, therefore, our problem becomes two dimensional. The generalized time-dependent Ginzburg-Landau equations in our case can be written as

$$\frac{u}{\sqrt{1 + \gamma^2 |\psi|^2}} \left(\frac{\partial}{\partial t} + \frac{\gamma^2}{2} \frac{\partial |\psi|^2}{\partial t} \right) \psi = (\nabla - i\mathbf{A})^2 \psi + (1 - |\psi|^2) \psi, \quad (1a)$$

$$\frac{\partial \mathbf{A}}{\partial t} = \text{Re}[\psi^* (-i\nabla - \mathbf{A})\psi] - \kappa^2 \text{rot rot } \mathbf{A}, \quad (1b)$$

where the parameter $\gamma = 2\tau_{in}\Delta(T)/\hbar$ is the product of the inelastic collision time τ_{in} for electron-phonon scattering and $\Delta(T) = 4k_B T_c u^{1/2} / \pi \sqrt{1 - T/T_c}$ is the value of the order parameter at temperature T , which follows from Gor'kov's derivation²⁷ of the Ginzburg-Landau equations. In Eqs. (1a) and (1b), the physical quantities are measured in dimensionless units: temperature in units of the critical temperature T_c , the vector potential $\mathbf{A} = (A_x, A_y, 0)$ and the momentum of the superconducting condensate $\mathbf{p} = \nabla\phi - \mathbf{A}$ are scaled in units $\Phi_0/[2\pi\xi(T)]$ (where Φ_0 is the quantum of magnetic flux), the order parameter $\psi = |\psi|e^{i\phi}$ in units of $\Delta(T)$, and the coordinates are in units of the coherence length $\xi(T) = [8k_B(T_c - T)/\pi\hbar D]^{-1/2}$. Time is scaled in units of the Ginzburg-Landau relaxation time $\tau_{GL} = \pi\hbar/8k_B(T_c - T)u$, and voltage (V) is in units of $\varphi_0 = \hbar/2e\tau_{GL}$ (σ_n is the normal-state conductivity). In these units, the magnetic field is scaled with $H_{c2} = \Phi_0/2\pi\xi^2$ and the current density with $j_0 = \sigma_n\hbar/2e\tau_{GL}\xi$. Following Ref. 25, the parameter u is taken to be equal to 5.79.

Instead of the usual gauge $\text{div } \mathbf{A} = 0$, we chose the electrostatic potential equal to zero $\varphi = 0$. The semi-implicit algorithm was used,²⁸ which provides an effective numerical solution of Eqs. (1a) and (1b) for the case of large values of the Ginzburg-Landau parameter κ . We apply periodic boundary conditions in the y direction, $\psi(y) = \psi(y+L)$, $\mathbf{A}(y) = \mathbf{A}(y+L)$ (

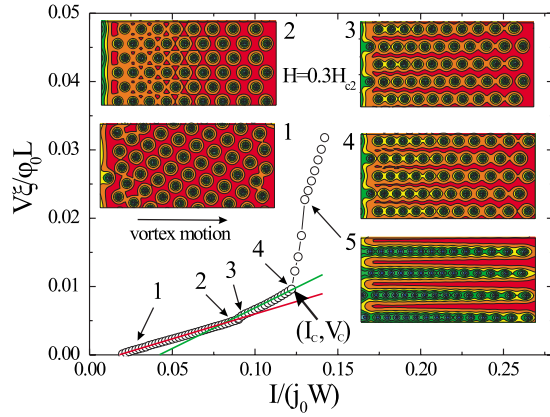


FIG. 2. (Color online) Current-voltage characteristics of the superconducting slab with width $W=50\xi$, $\gamma=10$, and $H=0.3H_{c2}$. Current increases from zero to some finite value. In the inset, snapshots of the order parameter at different values of the applied current are shown.

L is the period—see Fig. 1), and the superconductor-vacuum boundary conditions in the x direction, $(\nabla_x - iA_x)\psi|_{x=0,W}=0$. The transport current was introduced via the boundary condition for the vector potential in the x direction, $\text{rot } \mathbf{A}|_z(x=0,W)=H \pm H_J$, where $H_J=2\pi I/c$ is the magnetic field induced by the current I (per unit length in the z -direction) and H is the applied magnetic field. In all our calculations, we chose $\kappa=5$ and the parameter γ is varied from 0 to 40.

Due to the discrete nature of the vortex motion, the voltage response in our system is a time-dependent variable. We average it over a finite time interval which is taken to be larger than the period of the voltage variation. However, this time interval can be comparable to the switching time between different dynamic phases and it smoothens the current-voltage characteristics at the transition points.

III. REARRANGEMENT OF THE VORTEX LATTICE

First, we consider the situation when the applied magnetic field is larger than the magnetic field due to the transport current $H \gg H_J$. Therefore, the current density distribution is almost uniform over the width of the superconductor and it simplifies the analysis of the obtained numerical results. In Fig. 2, we present the current-voltage (I - V) characteristic of our system ($W=50\xi$, $L=25\xi$, and $\gamma=10$) under investigation at $H=0.3H_{c2}$. Vortex flow starts at some finite current I_s (due to the presence of the surface barrier in the system), and the vortex structure is close to the triangular lattice. With increasing current, it transforms to a rowlike structure but keeping the triangular ordering (see point 2 in Fig. 2). Increasing the current (arrow 3 in Fig. 3), there is a transition in the vortex structure which is visible as a kink in the I - V characteristic. The number of vortex rows decreases (from 6 to 5 in this particular case) and the number of vortices in the rows increases. Note that the number of vortices in the system does not change and the kink in the I - V characteristic is connected with a faster vortex motion in this vortex configuration. At the current indicated by arrow 4, there is a second

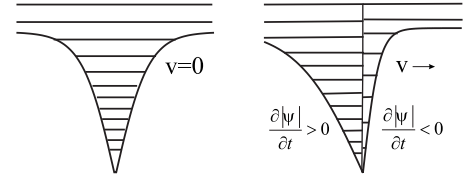


FIG. 3. Deformation of the vortex core due to vortex motion (schematic). The density of the horizontal lines shows the density of the quasiparticles. In case the diffusion length L_{in} is smaller than the coherence length $\xi(T)$, diffusion of the quasiparticles is not strong and locally there is an effective cooling and heating of the quasiparticles.

transition where the number of rows decreases further (from 5 to 4) and the distance between the vortices in each row decreases. Simultaneously, the vortex velocity increases steeply and we have a transition to a state with a much larger voltage.

The transitions in the vortex lattice will be explained by the modification of the shape of the vortex core due to non-equilibrium processes. Indeed, the motion of the vortex means a suppression of the order parameter in front of the vortex and recovering the order parameter behind it (see Fig. 3). If the vortex velocity is large enough ($v \lesssim \xi/\tau_{in}$), the number of quasiparticles in front of the vortex will be less than the equilibrium value and larger behind the vortex due to the finite relaxation time τ_{in} of the quasiparticle distribution function. Effectively, we have a cooling of the quasiparticles in front of the vortex and heating behind the vortex (see Fig. 3). This effect is very similar to the behavior of a superconducting weak link at voltages $V \lesssim 1/\tau_{in}$ (Refs. 29–31) when there is a cooling at the decrease of the order parameter and a heating when the order parameter increases in the weak link. Because the relaxation time of the order parameter depends on the temperature as $\tau_{|\psi|} \sim 1/(T_c - T)$, we have a long healing time of the order parameter behind the vortex and a short time suppression of the order parameter in front of the vortex. It leads to an elongated shape of the vortex core with a point where $|\psi|=0$ shifted to the direction of the vortex motion. This is visible (see Fig. 2) for vortices close to the right side of the superconductor, where the current density and the vortex velocity are maximal.

When the transition from five to four vortex rows in the vortex lattice occurs, the distance between the vortices suddenly decreases. If the vortex velocity is large enough such that $v > v_c \sim a/\tau_{|\psi|}$ (a is the distance between vortices in the row), the order parameter does not have sufficient time to recover after every vortex passage in the row and $|\psi|$ will be strongly suppressed along the vortex trajectory. It speeds up the vortex motion because the time variation of $|\psi|$ depends on the value of $|\psi|$: $\tau_{|\psi|} \sim \gamma|\psi|\tau_{GL}$.³² This is the reason for a transition from slow to fast vortex motion (quasiphase slip line behavior) and a steep increase in the voltage at the point where the current is I_c and the voltage is V_c in Fig. 2.

At higher magnetic fields, the situation is similar to the case $H=0.3H_{c2}$, but, in addition, a transition to a state with vortex rows moving with different velocities is possible (see Fig. 4). When a fast vortex row [which we will further call a quasiphase slip line (PSL)] appears in the sample, the super-

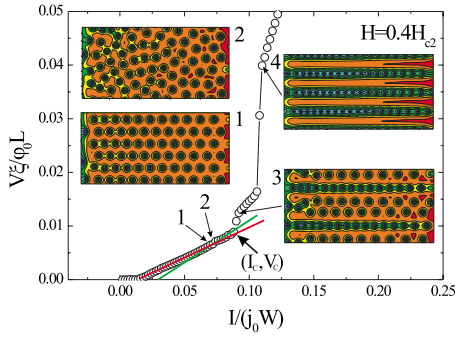


FIG. 4. (Color online) Current-voltage characteristics of the superconducting slab with width $W=50\xi$, $\gamma=10$, and $H=0.4H_{c2}$.

conducting current decreases around the PSL on the scale of the decay of the electric field E (or charge imbalance) L_E .⁴ Then, vortices in adjacent to PSL areas are forced to move with smaller velocities because the superconducting current mainly drives them. In the framework of the model equations [Eqs. (1a) and (1b)], $L_E \approx \sqrt{\gamma/uv\xi} > L_{in}$,³² and we indeed found that for larger values of γ , the current and magnetic field range over which this structure may exist increase. For example, for $\gamma=20$, the slow and fast vortex rows may coexist already at $H=0.3H_{c2}$, and for $\gamma=40$, they may coexist even at $H=0$.

Note that in contrast to the case $H=0.3H_{c2}$, the instability of the vortex lattice leads to quasichaotic vortex motion at currents between points 2 and 3. We relate this to the usage of periodic boundary conditions. For example, in case of $H=0.3H_{c2}$, the same chaotic behavior (not shown here) disappears between points 2 and 3 in Fig. 2 with an increase of the period of our system by a factor of 2 (with a small effect on the values of the currents where structural transitions occur). However, for $H=0.4H_{c2}$, doubling the period did not result in any effect.

We explain the influence of the boundary conditions by incommensurability effects between the period L and L_E . Actually the latter length defines the scale of the interaction between phase slip lines. Changing the parameter γ , we change L_E . For example, for $\gamma=20$ and $H=0.4H_{c2}$, we did not observe any irregular vortex distribution for the superconductor for the parameters corresponding to Fig. 3 even when $L=25\xi$.

At magnetic fields close to H_{c2} , there are also transitions in the vortex structures, but they are masked by a large num-

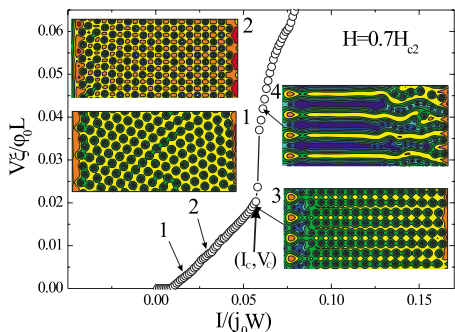


FIG. 5. (Color online) Current-voltage characteristics of the superconducting slab for the parameters of Fig. 2 and $H=0.7H_{c2}$.

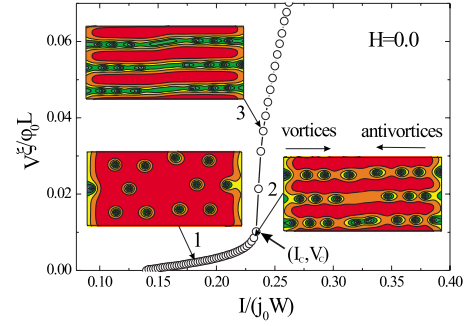


FIG. 6. (Color online) Current-voltage characteristics of the superconducting slab with the same parameters as in Fig. 2, but now for zero magnetic field.

ber of possible transitions due to the increased number of vortices in the system (see Fig. 5). The kinks in the current-voltage characteristics become almost invisible, and the jumps in the voltage gradually decreases at the current I_c where the quasiphase slip lines appear in the system.

IV. VORTEX MOTION AT ZERO MAGNETIC FIELD

In Fig. 6, we present the I - V characteristic of the same sample as in Fig. 2 at zero magnetic field. At low currents, we have slow vortex motion, while at large current, quasiphase slip lines appear. We should note that we did not observe any structural changes in the vortex lattice at low magnetic fields due to the small number of vortices and hence the large distance between them.

In case of zero magnetic field, the current density is strongly nonuniform over the width of the sample (see Fig. 7). When the current exceeds the critical value I_s (current of suppression of the surface barrier for vortex entry), the Meissner state is destroyed, and vortices and antivortices enter the sample, pass through it, and annihilate in the center. This process results in the appearance of an additional maximum in the current density in the center of the sample—see Fig. 7 (in agreement with analytical calculations of Refs. 33 and 34). For sample parameters of Fig. 6, the quasiphase slip behavior starts when the current density in the center reaches

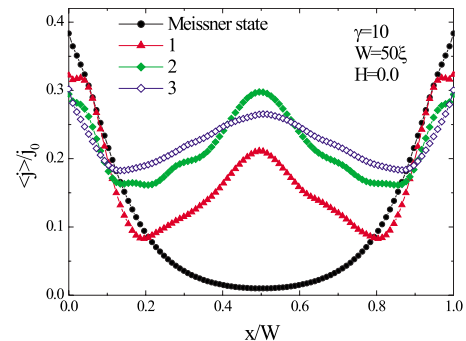


FIG. 7. (Color online) Distribution of the time and length averaged current density $\langle j \rangle = j_n + j_s$ over the width of the superconducting slab at zero magnetic field and different values of the transport current. Numbers 1–3 in the figure correspond to different values of the transport current in Fig. 6.

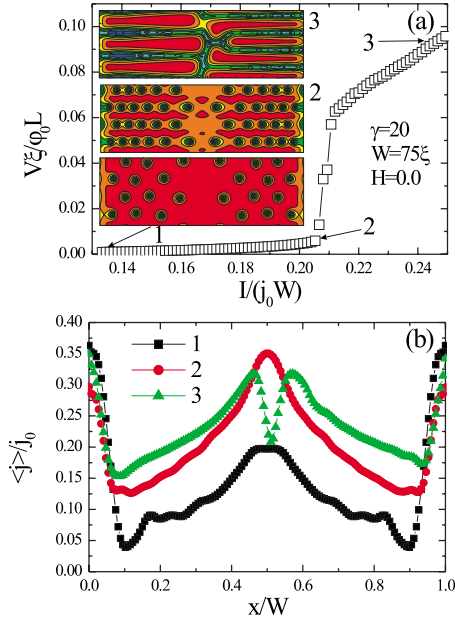


FIG. 8. (Color online) (a) Current-voltage characteristics of the superconducting slab with parameters $\gamma=20$ and $W=75\xi$ at zero magnetic field. In the inset in (a), we present snapshots of $|\psi|$ at different values of the current. (b) Distribution of the time and length averaged current density $\langle j \rangle = j_n + j_s$ for wider sample. Numbers correspond to different values of the current in (a).

the value close to the depairing current density j_{dep} . We found that at this moment, the annihilation of vortex-antivortex pairs speeds up and it provides a favorable condition for fast vortex motion across the whole sample. However, with increasing width of the sample, the transition to the fast vortex motion behavior starts at a larger current (see Fig. 8). As the speed of the fleet is defined by the speed of the slowest ship, the nucleation of the quasiphase slip line depends on the vortex motion in the place where the current density is minimal. When we increase the width of the sample, we decrease the minimal current density j_{min} in the sample [compare Figs. 8(b) and 7]. When j_{min} reaches the critical value, the quasiphase slip line nucleates in the sample. This critical value is smaller the larger γ . This result is closely connected with the findings of Ref. 32 where it was shown that the phase slip process does not exist in a quasi-one-dimensional superconductor and two-dimensional thin superconducting films with uniform distribution of the current density³⁵ if the current density is smaller than some critical value $j_{c1}(\gamma)$.

We like to stress that we did not find that the vortices and antivortices can pass through each other as predicted in Ref. 36. Probably, the uniform current distribution used in Ref. 36 is essential to observe this effect.

V. DISCUSSION

A. Comparison with other theoretical works

Our results strongly support the intuitive idea (published already in Ref. 20) about nucleation of phase slip lines at large currents against a background of vortex flow. This idea

was further developed in the theoretical work³⁷ where the current-voltage characteristics of a wide superconducting film with both viscous vortex flow and phase slip lines were calculated. However, the author used equations that are averaged over the intervortex distance and did not find the rearrangements of the vortex structure at high vortex velocities.

In Ref. 38, the appearance of the wake behind the moving vortex was theoretically predicted on the basis of an analytical solution of the linearized equation [Eq. (1a)] for the absolute value of the order parameter. Actually, such a wake should exist even in the simple time-dependent Ginzburg-Landau equation (with $\gamma=0$) due to the finite time for the order parameter relaxation $\tau_{|\psi|} \sim \tau_{GL}$. Indeed, when a vortex moves, the current density in front of its motion is the sum of the current density from the vortex j_{vort} and the transport current density j_{ext} , and likewise behind the vortex, it is the difference $j_{vort} - j_{ext}$. The time relaxation of the order parameter depends on the value of the current density if j is close to the depairing current, density (the larger the current the smaller is $\tau_{|\psi|}$ —see Chap. 11.4 in Ref. 4). If j_{ext} is close to j_{dep} , the difference between $\tau_{|\psi|}$ in front and behind the moving vortex is substantial,³⁹ and the moving vortex becomes elongated in the direction of its motion.

The change in the shape of the vortex was also found in Ref. 40 on the basis of a numerical solution of the 2D time-dependent Ginzburg-Landau equations. Such vortices were called kinematic vortices due to their high velocity. They were found to exist when a quasiphase slip line nucleated in the sample. The system resembles a Josephson vortex in a long Josephson junction where anisotropy is connected with different penetration depths of the screening current along and across the Josephson junction (see Chap. 6.4 in Ref. 4). In case of a phase slip line, the anisotropy is connected with a strongly suppressed order parameter in the direction of the vortex motion (along the quasiphase slip line).

In both of the above works, the dependence of the relaxation time $\tau_{|\psi|}$ on the value of the order parameter was ignored. In Ref. 40, the term $\gamma^2 \partial |\psi|^2 / 2 \partial t$ on the left hand side of Eq. (1a) was neglected, and instead of the coefficient $u / \sqrt{1 + \gamma^2 |\psi|^2}$, the variable parameter u^* was used.⁴⁰ Actually, in Ref. 38, the same approach was used because in Eq. (1a), a fixed value for the order parameter $|\psi|$ in the term $\tau_{|\psi|} = \tau_{GL} u \sqrt{1 + \gamma^2 |\psi|^2}$ was put.

However, in a TDGL model with $\gamma=0$ and arbitrary value of u , we did not find any steep transition from slow vortex flow to fast vortex motion (quasiphase slip line) at finite value of the applied magnetic field. The reason is simple: in that model, the relaxation time of the order parameter practically does not depend on the value of the order parameter and the mechanism of the switching in vortex motion discussed in Sec. III does not work. Besides, we did not find any vortex structure rearrangement in the model with $\gamma=0$ and arbitrary u . Probably, the change of the shape of the vortex is small in the above simplified model.

In Ref. 35, Eq. (1a) was coupled with the equation for the electrostatic potential and the transition from the slow vortex flow to the quasiphase slip lines behavior was numerically observed in case of thin 2D superconducting films of finite length in a perpendicular magnetic field. However, the rear-

rearrangement of the vortex lattice and the coexistence of the fast and slow vortex motions were not found because of the small width of the samples.

B. Range of validity of the obtained results

Our results are strictly valid only when $L_{in} < \xi(T)$, while usually, in experiments, $L_{in} \gg \xi(T)$. However, it is obvious that cooling and heating of the quasiparticles around the vortex core occur in both limits. Large L_{in} provides some kind of space averaging of these different processes (due to diffusion of the nonequilibrium quasiparticles from the overheated region to the overcooled one). In the framework of the LO theory, the zero order effect was calculated (when the dependence on the direction of the vortex motion was neglected), which roughly leads to an effective cooling of the system and a symmetrical shrinkage of the vortex core if the distance between the vortices is much smaller than L_{in} . In this limit, the separation of the system into slow moving vortices and quasiphase slip lines is, in principle, possible for $v > v_c$ when the vortex motion becomes unstable. The origin for such a behavior is the presence of the normal component of the current density (electric field) and its finite decay length from the phase slip line L_E . The slow vortex motion between the quasiphase slip line may occur due to a weakening of the superconducting component of the current near the quasiphase slip line. In the LO theory, this effect was neglected and only deviations of the longitudinal part of the quasiparticle distribution function from equilibrium were taken into account, while the transverse (even in energy) part of $f(E)$ is responsible for the appearance of the finite normal current in the superconductor.⁴

The situation is different if the distance between the vortices exceeds L_{in} and the effective averaging becomes weaker. The anisotropy of the vortex core and the effective attraction between vortices should be more pronounced and lead to the appearance of vortex rows and/or lines (slow or fast) even at vortex velocities less than v_c .

C. Comparison with experiments

The important property which follows from our calculations is the weak dependence of the critical voltage $V = V_c$ on the applied magnetic field (see inset in Fig. 9). We explained it by the rearrangements of the vortex lattice when the vortex velocity approaches v_c . Because in this case we do not have a triangular vortex lattice, the distance between vortices in the rows will be smaller than $a \sim \sqrt{\Phi_0/B}$ and defined by $a \sim 1/B$ dependence. Indeed, at current $I = I_c$, the transition to a state with four quasiphase slip lines occurs (see Figs. 2, 4, and 5) in the magnetic field range 0.3–0.7 H_{c2} , while the number of the vortices in the sample increases linearly with magnetic field. Assuming that the transition to the fast vortex motion state occurs when the distance between the vortices in the row is equal to $a \sim 1/B \sim v_c \tau_{in} \gamma$ (see Sec. III), we obtain $v_c \sim 1/B \tau_{in} \gamma$ and the field-independent critical voltage $V_c = v_c B L$. Such a dependence was experimentally observed in Ref. 13 for both low and high-temperature superconductors in the low magnetic field regime where the vortex separation

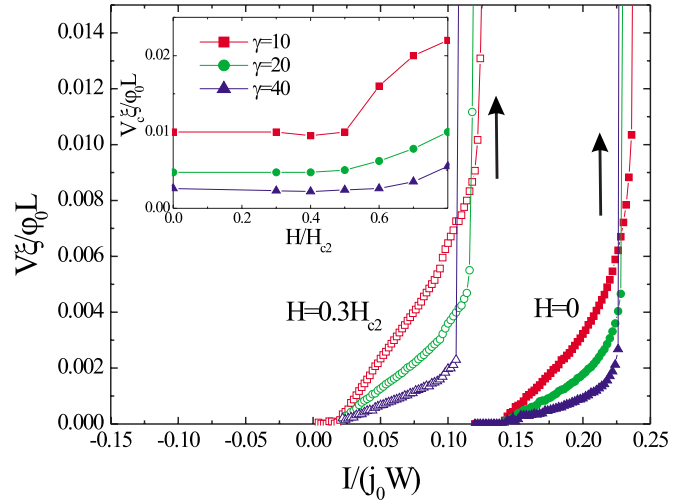


FIG. 9. (Color online) Current-voltage characteristics of the superconducting slab with width $W = 50\xi$, $\kappa = 5$, and different values of the parameter γ at two values of the magnetic field. In the inset, the dependence of the critical voltage on the magnetic field is shown for three values of the parameter $\gamma = 10, 20, 40$.

ration $a \gg L_{in}$ and the self-field of the transport current was negligible.

From the above estimations, it follows that $V_c \sim 1/\gamma$. We see from the inset in Fig. 9 that indeed $V_c \sim 1/\gamma$, and besides, the resistivity of the superconductor at low currents follows the dependence $\rho/\rho_n \sim 1/\gamma$ (see Fig. 9) analytically found in Ref. 41 for large magnetic fields in the temperature interval $T_c - \hbar/k_B \tau_{in} < T < T_c$, where Eqs. (1a) and (1b) are valid.

Our estimation of the critical velocity was made in the spirit of the paper of Doettinger *et al.*¹⁵ They supposed that the vortex motion instability occurs when the nonequilibrium quasiparticles induced in the vortex core do not have time to relax to equilibrium when the next vortex arrives to the place where they were induced, $\tau_{in} = a/v_c$. Actually, it means that the order parameter did not have time to increase [because its value depends on $f(E)$ and it cannot grow faster than τ_{in}].

The stairlike structure of the I - V characteristics (which is a fingerprint of the nucleation of the phase slip centers or quasiphase slip lines) was observed both in low- and high-temperature superconductors^{20–24} at low magnetic fields. In wide samples (in which the strongly nonuniform current density distribution over the width of the sample is realized in the Meissner state), a slow vortex motion was found at low currents, which is changed into the quasiphases slip line behavior at higher currents.^{20–23} It is interesting to note that the stairlike structure was also experimentally observed at high magnetic fields (and temperatures far below the critical one) in high-temperature superconductors.^{17,18} In this case, one was able to observe it only in the voltage driven regime.

In the experiments of Kunchur *et al.*,^{16–18} the quasiphase slip lines become visible because the penetration length of the electric field L_E increases in high magnetic field due to the suppression of the order parameter by vortices and a steep increase of τ_{in} at low temperatures.⁹ At low magnetic fields and high temperatures, too many quasiphase slip lines appear simultaneously at $I = I_c$ and it smoothes out the stair structure of the I - V characteristic.

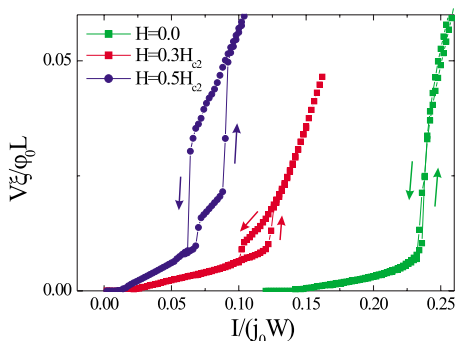


FIG. 10. (Color online) Hysteresis in the current-voltage characteristics of the superconducting slab with $W=50\xi$, $\gamma=10$, and different magnetic fields.

We explain the absence of the stairlike structure in the majority of the experiments where the LO effect was studied due to the large length of the samples as compared to L_E . At the instability point, many quasiphase slip lines should appear in such a sample, and it results into a large heating of the electronic subsystem and the sample itself. This could be the reason for the transition to the nearly normal state. Besides, in those samples, the role of the voltage can be very pronounced and it leads to an additional suppression of superconductivity, the effect which is absent in the model equations [Eqs. (1a) and (1b)].⁴² Therefore, it would be interesting to perform an experiment on a short superconducting bridge with length of about several L_E at different temperatures and magnetic fields. Taking into account the strong dependence of τ_{in} and hence L_E on temperature, it would be worth studying several samples with different lengths satisfying the condition $L \sim L_E$ at different temperatures. By variation of the magnetic field, one could observe the predicted splitting of the vortex flow into regions with fast vortex flow (quasiphase slip lines) and slow vortex flow. A good candidate is NbGe which has rather low bulk pinning even at $T \sim T_c/2$.⁷

D. Hysteretic behavior

The hysteresis is almost absent in zero magnetic field for a superconducting slab with $W=50$, $\kappa=5$, and $\gamma=10$ (see Fig. 10). Hysteresis appears when we increase the applied magnetic field (see Fig. 10) or decrease the width of the sample. In both cases, the current density distribution becomes more uniform in the sample and it brings hysteresis in the system.

The physical reason for this effect is as follows. Consider first the case of zero applied magnetic field $H=0$. In Refs. 32 and 35, it was found that in a superconductor with uniform current density distribution, the phase slip center and/or line does not exist at current density $j_{c1}(\gamma)$ which can be smaller than j_{dep} (in case of zero fluctuations). However, the superconducting state in such a system can be stable up to $I_c = j_{dep}dW$. When a quasiphase slip line nucleates at I_c , it can exist up to a smaller current $I_1 = j_{c1}dW$ and it leads to hysteretic behavior. When we take into account screening effects, the current density distribution becomes nonuniform over the

width of the sample. It is maximal on the edge and minimal in the center of the sample being in the Meissner state. At current $I = I_s < I_c$, the current density on the edge reaches the depairing current density and the superconducting state becomes unstable. Vortices enter the sample, and if the minimal current density is larger than j_{c1} , they move fast and form a quasiphase slip line. If the minimal current density is smaller than j_{c1} , they move slowly and form quasiphase slip lines at a larger current when the condition $j_{min} > j_{c1}$ is fulfilled. In the latter case, hysteresis is absent because the transition from the slow to the fast vortex motion (or vice versa) occurs when the current density in one point (over the width of the sample) reaches the critical value. It does not lead to a crucial redistribution of the normal and superconducting current densities over the sample and the vortex motion is almost nonhysteretic.

When a magnetic field is applied, the transition to the fast vortex motion occurs when the current density reaches a critical value (which depends on the magnetic field) practically over the whole sample. As a result, the distribution of the normal and superconducting current densities changes drastically over the whole sample, and it provides the hysteretic behavior for vortex motion in our model system.

In our calculations, we did not take into account heating effects. Their incorporation in the considered model will increase the hysteresis⁴³ and mask all effects⁴⁴ discussed in our paper.

E. Synchronization of vortex motion in adjacent vortex rows

Can the motion of the vortices in two adjacent quasiphase slip rows and/or lines be synchronized? It was found in many papers (for a review, see Refs. 45 and 46) that the dynamics of the order parameter in one phase slip center may influence the dynamics of the order parameter in a remote phase slip center even if the distance between them is large. The effect is mainly connected with the long decay length of the quasiparticle (normal) current from the phase slip center. As a result, the ac component of the normal current affects the oscillations of the order parameter in the other phase slip center in a way similar to a Josephson junction under the action of an external ac current or electromagnetic radiation. The interaction between phase slip centers becomes more complicated if one takes into account the nucleation of the charge imbalance waves,⁴⁵ which can both enhance and suppress the synchronization of the order parameter oscillations in adjacent phase slip centers and/or lines.⁴⁵

In our calculations, effects due to charge imbalance waves were not considered and quasiphase slip lines interact only via the ac component of the normal current. In Fig. 11, we present the time dependence of the averaged, over the length of the sample, electric field at the edge of the superconductor and the local electric field in the point where the quasiphase slip line at large current nucleates (at $H=0.3H_{c2}$ and different currents). At low currents, when the induced voltage and normal current are small, the motion of the vortices in adjacent rows is out of phase because of weak interactions between vortices and strong repulsion between vortices. On the contrary, at large currents, the exit of the vortices from the

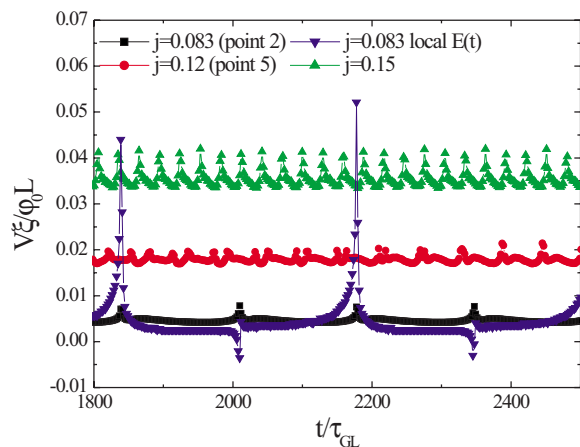


FIG. 11. (Color online) Time dependence of the instant voltage and local electric field at different values of the applied current for the sample with parameters as in Fig. 2.

superconductor in adjacent rows becomes in phase. It means that the emitted electromagnetic radiation should be considerably enhanced in this case in comparison with the low current limit.

The frequency of the radiation can be tuned by an applied magnetic field or/and by applied current. The applied magnetic field changes the number of the vortices in the row and hence changes the distance between vortices while transport current changes the vortex velocity. Both factors influence the frequency of the extracted radiation $\nu = v/a$. Taking typical values for the critical velocity in YBaCuO compounds at $T=77$ K and $B=1$ T, $v_c=10^3$ m/s (Ref. 9), and the intervortex distance $a \approx \sqrt{\Phi_0/B} = 40$ nm, we obtain $\nu \approx 4 \times 10^{11}$ Hz. In the quasiphase slip line regime, the vortex velocity $v \gg v_c$ and the frequency approaches the terahertz regime.

VI. CONCLUSIONS

In the framework of the generalized time-dependent Ginzburg-Landau equations, we showed that with increasing applied current, the moving Abrikosov vortex lattice changes its structure from a triangular one to a set of parallel vortex rows. The effect originates from changes in the shape of the moving vortex. The vortex core becomes elongated in the

direction of vortex motion because of different relaxation times of the order parameter in front and behind the moving vortex. In front of the moving vortex, the order parameter may vary very fast due to a large value of the local current density and a deficit of quasiparticles in comparison with its equilibrium value. On the contrary, the number of the quasiparticles exceeds locally their equilibrium value, and the current density is small behind the moving vortex and it increases the relaxation time of the order parameter. This results in the appearance of a wake behind the vortex which attracts other vortices.

We found that the rearrangement of the vortex lattice results in field-independent values of the critical voltage at which the transition to the state with quasiphase slip lines occurs. This is connected with changes of the intervortex distance at the structural transitions of the vortex lattice. In a triangular lattice, the average distance between vortices varies as $a \sim 1/\sqrt{B}$, while in the case of vortex rows, the minimal intervortex distance decreases with increasing magnetic field as $a \sim 1/B$. It results in the dependence $V_c \sim \sqrt{B}$ for triangular lattice and $V_c \sim \text{const}$ for vortex rows.

At some magnetic field, the quasiphase slip lines can coexist with slowly moving vortices between such lines. Besides, we found that the motion of the vortices in adjacent quasiphase slip lines can be synchronized at large vortex velocity $v > v_c$. Both effects are possible due to the long decay length of the normal current near the quasiphase slip line. It decreases the superconducting component of the current in the system and provides synchronization of oscillations in the order parameter at the quasiphase slip lines.

Although our results are strictly valid when $\xi(T) > L_{in}$, they qualitatively explain experiments on the instability of the vortex flow at low magnetic fields when the distance between vortices $a \gg L_{in} \gg \xi(T)$. Besides, our results support the idea that a similar instability of the vortex lattice should exist for $v > v_c$ even when $a < L_{in}$.

ACKNOWLEDGMENTS

We thank V. V. Kurin for useful discussions. This work was supported by the Flemish Science Foundation (FWO-VI), the Belgian Science Policy (IAP), and the ESF-AQDJJ program. D.Y.V. acknowledges support from INTAS (04-83-3139) and the Dynasty Foundation.

*vodolazov@ipm.sci-nnov.ru

†francois.peeters@ua.ac.be

¹A. I. Larkin and Yu. N. Ovchinnikov, Zh. Eksp. Teor. Fiz. **68**, 1915 (1975) [Sov. Phys. JETP **41**, 960 (1976)].

²A. I. Larkin and Yu. N. Ovchinnikov, in *Nonequilibrium Superconductivity*, edited by D. N. Langenberg and A. I. Larkin (Elsevier, Amsterdam, 1986), Chap. 11.

³W. Klein, R. P. Huebener, S. Gauss, and J. Parisi, J. Low Temp. Phys. **61**, 413 (1985).

⁴M. Tinkham, *Introduction to Superconductivity* (McGraw-Hill, New York, 1996).

⁵L. E. Musienko, I. M. Dmitrenko, and V. G. Volotskaya, Pis'ma Zh. Eksp. Teor. Fiz. **31**, 603 (1980) [JETP Lett. **31**, 567 (1980)].

⁶F. Lefloch, C. Hoffmann, and O. Demolliens, Physica C **319**, 258 (1999).

⁷D. Babić, J. Bentner, C. Sürgers, and C. Strunk, Phys. Rev. B **69**, 092510 (2004).

⁸A. V. Samoilov, M. Konczykowski, N. C. Yeh, S. Berry, and C. Tsuei, Phys. Rev. Lett. **75**, 4118 (1995).

⁹S. G. Doettinger, R. P. Huebener, R. Gerdemann, A. Kuhle, S. Anders, T. G. Trauble, and J. C. Villegier, Phys. Rev. Lett. **73**, 1691 (1994).

- ¹⁰S. G. Doettinger, S. Kittelberger, R. P. Huebener, and C. C. Tsuei, *Phys. Rev. B* **56**, 14157 (1997).
- ¹¹Z. L. Xiao and P. Ziemann, *Phys. Rev. B* **53**, 15265 (1996).
- ¹²Z. L. Xiao, P. Voss-de Haan, G. Jakob, Th. Kluge, P. Haibach, H. Adrian, and E. Y. Andrei, *Phys. Rev. B* **59**, 1481 (1999).
- ¹³J. Chiaverini, J. N. Eckstein, I. Bozovic, S. Doniach, and A. Kapitulnik, arXiv:cond-mat/0007479 (unpublished).
- ¹⁴J. Bardeen and M. J. Stephen, *Phys. Rev.* **140**, A1197 (1965).
- ¹⁵S. G. Doettinger, R. P. Huebener, and A. Khule, *Physica C* **251**, 285 (1995).
- ¹⁶M. N. Kunchur, *Phys. Rev. Lett.* **89**, 137005 (2002).
- ¹⁷M. N. Kunchur, B. I. Ivlev, and J. M. Knight, *Phys. Rev. Lett.* **87**, 177001 (2001).
- ¹⁸M. N. Kunchur, B. I. Ivlev, and J. M. Knight, *Phys. Rev. B* **66**, 060505(R) (2002).
- ¹⁹S. G. Doettinger, R. P. Huebener, and S. Kittelberger, *Phys. Rev. B* **55**, 6044 (1997).
- ²⁰V. G. Volotskaya, I. M. Dmitrenko, L. E. Musienko, and A. G. Sivakov, *Fiz. Nizk. Temp.* **7**, 383 (1981) [*Sov. J. Low Temp. Phys.* **7**, 168 (1981)].
- ²¹V. G. Volotskaya, I. M. Dmitrenko, and A. G. Sivakov, *Fiz. Nizk. Temp.* **10**, 347 (1984) [*Sov. J. Low Temp. Phys.* **10**, 179 (1984)].
- ²²V. M. Dmitriev, I. V. Zolochevskii, T. V. Salenkova, and E. V. Khristenko, *Low Temp. Phys.* **31**, 127 (2005).
- ²³S. G. Zybtssev, I. G. Gorlova, and V. Ya. Pokrovski, *JETP Lett.* **74**, 168 (2001).
- ²⁴A. G. Sivakov, A. M. Glukhov, A. N. Omelyanchouk, Y. Koval, P. Müller, and A. V. Ustinov, *Phys. Rev. Lett.* **91**, 267001 (2003).
- ²⁵L. Kramer and R. J. Watts-Tobin, *Phys. Rev. Lett.* **40**, 1041 (1978).
- ²⁶R. J. Watts-Tobin, Y. Krähenbühl, and L. Kramer, *J. Low Temp. Phys.* **42**, 459 (1981).
- ²⁷L. P. Gor'kov, *Zh. Eksp. Teor. Fiz.* **36**, 1918 (1959) [*Sov. Phys. JETP* **9**, 1364 (1959)].
- ²⁸T. Winiacki and C. S. Adams, *J. Comput. Phys.* **179**, 127 (2002).
- ²⁹A. Schmid, G. Schon, and M. Tinkham, *Phys. Rev. B* **21**, 5076 (1980).
- ³⁰A. A. Golub, *Zh. Eksp. Teor. Fiz.* **71**, 341 (1976) [*Sov. Phys. JETP* **44**, 178 (1976)].
- ³¹L. G. Aslamazov and A. I. Larkin, *Zh. Eksp. Teor. Fiz.* **70**, 1340 (1976) [*Sov. Phys. JETP* **43**, 698 (1976)].
- ³²S. Michotte, S. Matefi-Tempfli, L. Piraux, D. Y. Vodolazov, and F. M. Peeters, *Phys. Rev. B* **69**, 094512 (2004).
- ³³L. G. Aslamazov and S. V. Lempitsky, *Zh. Eksp. Teor. Fiz.* **84**, 2216 (1983) [*Sov. Phys. JETP* **57**, 1291 (1983)].
- ³⁴B. Yu. Blok and S. V. Lempitskii, *Fiz. Tverd. Tela (Leningrad)* **26**, 457 (1984) [*Sov. Phys. Solid State* **26**, 272 (1984)].
- ³⁵D. Y. Vodolazov, B. J. Baelus, and F. M. Peeters, *Physica C* **404**, 400 (2004).
- ³⁶A. Weber and L. Kramer, *J. Low Temp. Phys.* **84**, 289 (1991).
- ³⁷S. V. Lempitskii, *Zh. Eksp. Teor. Fiz.* **90**, 793 (1986) [*Sov. Phys. JETP* **63**, 462 (1986)].
- ³⁸L. I. Glazman, *Fiz. Nizk. Temp.* **12**, 688 (1986) [*Sov. J. Low Temp. Phys.* **12**, 389 (1986)].
- ³⁹The relaxation time behind the moving vortex could be estimated from the work of Glazman (Ref. 38) if we replace the time τ_{in} by τ_{GL} in his results.
- ⁴⁰A. Andronov, I. Gordion, V. Kurin, I. Nefedov, and I. Shereshevsky, *Physica C* **213**, 193 (1993).
- ⁴¹A. I. Larkin and Yu. N. Ovchinnikov, *Zh. Eksp. Teor. Fiz.* **73**, 299 (1977) [*Sov. Phys. JETP* **46**, 155 (1976)].
- ⁴²D. Y. Vodolazov and F. M. Peeters, arXiv:cond-mat/0611315 (unpublished).
- ⁴³A. I. Bezuglij and V. A. Shklovskij, *Physica C* **202**, 234 (1992).
- ⁴⁴D. Y. Vodolazov, F. M. Peeters, M. Morelle, and V. V. Moshchalkov, *Phys. Rev. B* **71**, 184502 (2005).
- ⁴⁵A. M. Kadin and A. M. Goldman, in *Nonequilibrium Superconductivity*, edited by D. N. Langenberg and A. I. Larkin (Elsevier Science, Berlin, 1986), p. 254.
- ⁴⁶R. Tidecks, *Current-Induced Nonequilibrium Phenomena in Quasi-one-dimensional Superconductors* (Springer, Berlin, 1990), p. 269.